Submarine Gas Hydrate Reservoir Simulations – A Gas/Liquid Fluid Flow Model for Gas Hydrate Containing Sediments

S. Schlüter*[1], T. Hennig[1], G. Janicki[1], G. Deerberg[1]
[1]Fraunhofer Institute for Environmental, Safety and Energy Technology UMSICHT
*Osterfelder Str. 3, D-46045 Oberhausen, stefan.schlueter@umsicht.fraunhofer.de

Abstract: In the medium term, gas hydrate reservoirs in the subsea sediment are intended as deposits for CO_2 from fossil fuel consumption. This idea is supported by the thermodynamics of CO_2 and methane hydrates and the fact, that CO_2 hydrates are more stable than methane hydrates in a certain *P-T* range. The potential of producing methane by depressurization and/or by injecting CO_2 is numerically studied in the frame of the research project *SUGAR*. Here, a numerical model for the production of natural gas from submarine gas hydrate reservoirs based on a 2-phase Darcy flow in a sediment/hydrate matrix is described. The model was implemented in *COMSOL* with BDF time stepping and a fully coupled solution approach. Simulation cases presented and discussed here are the depressurization of a methane hydrate bearing reservoir at varied layer disposals and a depressurization with simultaneous injection of CO_2 by a second injection well.

Keywords: methane hydrate, reservoir simulation, two-phase flow, CO_2 sequestration

1. Introduction

Gas hydrates are non-stoichiometric, ice-like compounds of water and gas molecules which are stable at low temperature and elevated pressure [1-3]. Generally, gas hydrates can contain various guest molecules. Besides methane, carbon dioxide, hydrogen sulphide and seldom carbons are involved. Much more than 90% of natural gas hydrates in the terrestrial system are methane hydrates which exist in submarine sediments and in permafrost soils.

The recovery of methane from submarine gas hydrate bearing sediments is considered to be a promising measure to overcome future shortages in natural gas. Due to appropriate stability conditions, methane recovery maybe well combined with CO_2 storage in form of hydrates.

In recent years, intense research has been focused on the simulation of natural gas exploitation from gas hydrate reservoirs. Besides the technical and economical efforts for drilling in submarine sediments, the challenges concern the reaction kinetics and transport resistances within the sediments in which gas hydrates are embedded in natural reservoirs.

Thus, to find the optimal strategy for the gas exploitation with or without CO_2 storage, a large variety of parameters describing the properties of particular target layers as well as time and position dependent thermodynamic conditions of hydrate/gas/water systems have to be considered.

2. Exploitation of gas hydrates

According to the thermodynamic equilibrium conditions of methane hydrate, in general four destabilization methods exist: thermal stimulation, depressurization, injection of inhibiting additives (to change the stability conditions) and the substitution of methane by another gas e. g. carbon dioxide. Different concepts to realize either one single of those mechanisms or a combination of different measures were developed theoretically and evaluated with respect to the boundary conditions already been identified in natural reservoirs.

Within the framework of the German *SUGAR* research project, strategies to recover methane from submarine gas hydrate reservoirs and simultaneously store CO_2 as hydrates are explored. Before undertaking drilling and production tests numerical simulations of the local and site specific processes are helpful and necessary. For this purpose, to describe the methane production from submarine hydrate reservoirs and the substitution of methane with CO_2, a new scientific simulation code called *HyReS* was developed and implemented in *COMSOL Multiphysics*.

3. Reservoir model equations

The basic conservation equations of the new developed reservoir model are the phase continuity equations,

$$\frac{\partial}{\partial t}\left(\phi S_G \rho_G\right) + \nabla\cdot\left(\rho_G \mathbf{u}_G\right) = s_G$$
$$\frac{\partial}{\partial t}\left(\phi S_L \rho_L\right) + \nabla\cdot\left(\rho_L \mathbf{u}_L\right) = s_L$$
$$\frac{\partial}{\partial t}\left(\phi S_{MH} \rho_{MH}\right) = s_{MH}$$
$$\frac{\partial}{\partial t}\left(\phi S_{CH} \rho_{CH}\right) = s_{CH}$$

the component mass balances in the gas and the liquid phase,

$$\phi S_G \frac{\partial c_{i,G}}{\partial t} + c_{i,G}\phi\frac{\partial S_G}{\partial t} + \nabla\cdot\left(-\phi S_G \boldsymbol{\delta}_{i,G}^{eff}\nabla c_{i,G} + c_{i,G}\mathbf{u}_G\right) = \tilde{s}_{i,G}$$
$$\phi S_L \frac{\partial c_{i,L}}{\partial t} + c_{i,L}\phi\frac{\partial S_L}{\partial t} + \nabla\cdot\left(-\phi S_L \boldsymbol{\delta}_{i,L}^{eff}\nabla c_{i,L} + c_{i,L}\mathbf{u}_L\right) = \tilde{s}_{i,L}$$

and the energy equations for gas, liquid, hydrate and sediment phases:

$$\phi S_G \rho_G c_{P,G}\frac{\partial T_G}{\partial t} + \nabla\cdot\left(-\phi S_G \boldsymbol{\lambda}_G \nabla T_G\right) + \rho_G c_{P,G}\mathbf{u}_G\nabla T_G = \phi S_G \beta_G T_G \frac{\partial P_G}{\partial t} - \mathbf{u}_G\left(1-\beta_G T_G\right)\nabla P_G + q_G$$

$$\phi S_L \rho_L c_{P,L}\frac{\partial T_L}{\partial t} + \nabla\cdot\left(-\phi S_L \boldsymbol{\lambda}_L \nabla T_L\right) + \rho_L c_{P,L}\mathbf{u}_L\nabla T_L = q_L$$

$$\phi\left(S_{MH}\rho_{MH}c_{P,MH} + S_{CH}\rho_{CH}c_{P,CH}\right)\frac{\partial T_H}{\partial t} - \nabla\cdot\left(\phi\left(S_{MH}\boldsymbol{\lambda}_{MH} + S_{CH}\boldsymbol{\lambda}_{CH}\right)\nabla T_H\right) = q_H$$

$$\left(1-\phi\right)\rho_S c_{P,S}\frac{\partial T_S}{\partial t} + \nabla\cdot\left(-\left(1-\phi\right)\boldsymbol{\lambda}_S\nabla T_S\right) = q_S$$

For the implementation in *COMSOL Multiphysics* some major modifications have been done on the main conservation equations. *Firstly*, the four phase energy balances are summarized to a single energy balance of the system with the unique dependent variable *T*. This is done by summarizing all energy equations together and eliminating the interphase heat transfer fluxes.

Secondly, the component mass balances for the gas phase are switched to molar fractions as dependent variable. The resulting equations are

$$\phi S_G \tilde{\rho}_G \frac{\partial y_i}{\partial t} + y_i \frac{\partial}{\partial t}(\phi S_G \tilde{\rho}_G) + \nabla\cdot\left(-\phi S_G \boldsymbol{\delta}_{i,G}^{eff}\tilde{\rho}_G \nabla y_i + \mathbf{u}_G y_i \tilde{\rho}_G\right) = \tilde{s}_{i,G}$$

with

$$\frac{\partial}{\partial t}(\phi S_G \tilde{\rho}_G) = \phi S_G \tilde{\rho}_G \left(\frac{1}{S_G}\frac{\partial S_G}{\partial t} + \chi_G \frac{\partial P_G}{\partial t} - \beta_G \frac{\partial T_G}{\partial t} + \sum_{i=1}^{n-1}\left(\varphi_{i,G} - \frac{\tilde{M}_i - \tilde{M}_n}{\tilde{M}_G}\right)\frac{\partial y_i}{\partial t}\right)$$

Thirdly, the continuity equations are further developed to get a numerically robust equation system for reservoir pressure *P* and saturation S_L (see [4, 5]). Therefore, the general continuity equation of a phase *j* is written as

$$\phi\frac{\partial S_j}{\partial t} + \phi S_j \frac{1}{\rho}\frac{\partial \rho_j}{\partial t} + \nabla\cdot\mathbf{u}_j + \mathbf{u}_j\cdot\left(\frac{\nabla\rho_j}{\rho_j}\right) = \frac{s_j}{\rho_j}$$

This form offers the important possibility to eliminate the time derivations of S_j by summarizing over all phases:

$$\sum_j S_j = 1\,, \quad \sum_j \frac{\partial S_j}{\partial t} = 0$$

A general form of Darcy's law is used to give an expression for the velocity fields $\mathbf{u}_G$ and $\mathbf{u}_L$:

$$\mathbf{u}_j = -\mathbf{K}_f \Lambda_j\left(\nabla P_j + \mathbf{g}\rho_j\right)$$

with

$$\Lambda_j = \frac{k_{rel,j}}{\eta_j}\,, \quad k_{rel,j} = f_j\left(\phi, S_H, S_L\right)$$

In compressible media density derivations must be taken into account in time and space; they are defined here as

$$\chi_j = \frac{1}{\rho_j}\left(\frac{\partial\rho_j}{\partial P_j}\right)_{T,y_i}\,, \quad \beta_j = -\frac{1}{\rho_j}\left(\frac{\partial\rho_j}{\partial T_j}\right)_{P,y_i}\,,$$
$$\varphi_{i,j} = \frac{1}{\rho_j}\left(\frac{\partial\rho_j}{\partial y_i}\right)_{P,T} \text{ or } \quad \varphi_{i,j} = \frac{1}{\rho_j}\left(\frac{\partial\rho_j}{\partial c_i}\right)_{P,T}$$

Hence, summarizing the continuity equations of all phases together, inserting the terms given above and rearrange, the pressure equation of the reservoir system is given by the following general form:

$$\phi\sum_j S_j\chi_j\frac{\partial P_j}{\partial t}+\nabla\cdot\left(-\mathbf{K}_f\sum_j\Lambda_j\left(\nabla P_j+\mathbf{g}\rho_j\right)\right)$$
$$-\mathbf{K}_f\sum_j\Lambda_j\begin{pmatrix}\chi_j\left(\nabla P_j+\mathbf{g}\rho_j\right)-\beta_j\nabla T\\+\sum_k\varphi_{k,j}\nabla y_{k,j}\end{pmatrix}\nabla P_j=$$
$$\sum_j\frac{s_j}{\rho_j}+\phi\sum_j S_j\left(\beta_j\frac{\partial T}{\partial t}-\sum_i\varphi_{i,j}\frac{\partial y_{i,j}}{\partial t}\right)$$
$$-\mathbf{K}_f\mathbf{g}\sum_j\Lambda_j\rho_j\left(\beta_j\nabla T-\sum_i\varphi_{i,j}\nabla y_{i,j}\right)$$

The term in the flow divergence can be recognized as the sum of all phase velocities, so this form of the reservoir pressure equation is sometimes called as the *total velocity equation*. Mathematically, Darcy's law leads to a strong diffusion in pressure, and due to eliminating the $\partial S_j/\partial t$ terms, this equation is numerically robust and well to handle with *COMSOL* solvers. But in the case of two-phase flow a *second* equation is necessary for either the gas or the liquid phase saturation. Due to lower phase velocities the liquid phase saturation is used:

$$\phi\frac{\partial S_L}{\partial t}+\phi S_L\chi_L\frac{\partial P_L}{\partial t}+\nabla\cdot\begin{pmatrix}-\varepsilon\nabla S_L\\-\mathbf{K}_f\Lambda_L\left(\nabla P_L+\mathbf{g}\rho_L\right)\end{pmatrix}$$
$$-\mathbf{K}_f\Lambda_L\begin{pmatrix}\chi_L\left(\nabla P_L+\mathbf{g}\rho_L\right)-\beta_L\nabla T\\+\sum_i\varphi_{i,L}\nabla c_{i,L}\end{pmatrix}\nabla P_L=$$
$$\frac{s_L}{\rho_L}+\phi S_L\left(\beta_L\frac{\partial T}{\partial t}-\sum_i\varphi_{i,L}\frac{\partial c_{k,L}}{\partial t}\right)$$
$$-\mathbf{K}_f\mathbf{g}\Lambda_L\rho_L\left(\beta_j\nabla T-\sum_i\varphi_{i,L}\nabla c_{i,L}\right)$$

For numerical stabilization an artificial diffusion in S_L with a diffusion coefficient ε must be introduced here to get a robust solution process. The two hydrate saturation equations for S_{MH} and S_{CH} do not contain any flow velocity fields, so they can be solved as ODE's independently of the pressure and saturation equations:

$$\phi\frac{\partial S_{MH}}{\partial t}+\phi S_{MH}\left(\chi_{MH}\frac{\partial P_L}{\partial t}-\beta_{MH}\frac{\partial T}{\partial t}\right)=\frac{s_{MH}}{\rho_{MH}}$$
$$\phi\frac{\partial S_{CH}}{\partial t}+\phi S_{CH}\left(\chi_{CH}\frac{\partial P_L}{\partial t}-\beta_{CH}\frac{\partial T}{\partial t}\right)=\frac{s_{CH}}{\rho_{CH}}$$

In porous media pressure differences between gas and liquid phase occur due to capillary effects, which must be taken into account. The capillary pressure is defined as

$$P_C=P_G-P_L\quad\text{with}\quad P_C=f\left(\phi,S_L,S_H,\ldots\right)$$

Setting the dependent variable P to P_G, the gas and liquid phase pressures and their derivations can be expressed by P and P_C:

$$P=P_G,\quad P_L=P-P_C$$
$$\nabla P_G=\nabla P,\quad \nabla P_L=\nabla P-\nabla P_C$$
$$\frac{\partial P_G}{\partial t}=\frac{\partial P}{\partial t},\quad \frac{\partial P_L}{\partial t}=\frac{\partial P}{\partial t}-\frac{\partial P_C}{\partial t}$$

Substitution of phase pressures and their time and space derivations by these expressions gives the final form of the balance equation system.

The source terms in the conservation equations arise from hydrate (de)composition and gas absorption effects. For the reservoir model the following expressions are applied for the *mass volume sources*,

$$s_G=-R_{MH}\tilde{M}_M-R_{CH}\tilde{M}_C-\sum_i\tilde{s}_{i,L}\tilde{M}_i$$
$$s_L=-\left(\nu_{MH}R_{MH}+\nu_{CH}R_{CH}\right)\tilde{M}_W+\sum_i\tilde{s}_{i,L}\tilde{M}_i$$
$$s_{MH}=R_{MH}\tilde{M}_{MH}$$
$$s_{CH}=R_{CH}\tilde{M}_{CH}$$
$$\tilde{s}_{M,G}=-R_{MH}-\tilde{s}_{M,L},\ \tilde{s}_{M,L}=\psi_L a_{GL}\left(c^*_{M,L}-c_{M,L}\right)$$
$$\tilde{s}_{C,G}=-R_{CH}-\tilde{s}_{C,L},\ \tilde{s}_{C,L}=\psi_L a_{GL}\left(c^*_{C,L}-c_{C,L}\right)$$

and for the *energy volume sources* (here for the summarized energy equation):

$$q=-R_{MH}\Delta h_{MH}-R_{CH}\Delta h_{CH}+\sum_i\tilde{s}_{i,L}\Delta h_{abs,i}$$

The initial and boundary conditions to solve these equations depends on the geological and technical scenario for a specific reservoir simulation case. In general, flux conditions hold for mass fluxes leaving or entering the domain. The pressure condition, which holds for a depressurization of the domain by a well at a certain pressure, is set by a *weak constraint* boundary condition in the pressure/saturation interface. The advantages of this setting are a better numerical stability of the solution process and an accurate expression for the phase velocities at the well boundary via the Lagrange multiplier.

These equations are implemented with *COMSOL Multiphysics* in a 2-d axisymmetric model and a general 3-d Cartesian axis model. The specific model equations and space dimensions depend on the reservoir scenario, its physics and its symmetries, but in most cases the equation system is very similar to the basic equations given here. Created meshes are based on mapped structures in 2-d and on free tetrahedral structures or triangular surface structures swept in vertical direction in 3-d.

The *COMSOL implementation* is mainly equation based using the *Coefficient Form PDE* interface for hydrate bearing domains. The pressure and saturation equations are implemented together in one interface, just as the component equations for the gas phase (methane and carbon dioxide) and the component equations for the liquid phase (methane, carbon dioxide and salt). Hydrate saturation of methane and carbon dioxide are given as a *Domain ODE* interface; the capillary pressure equation is set in a *Domain DAE* interface to have fast access to its derivatives. Only the energy equation is implemented in an interface pre-arranged by *COMSOL*, namely the *Heat Transfer in Porous Media* interface (it requires the *Heat Transfer* module). *Discretization* is set to default conditions in all interfaces. The time dependent solver is set up in fully coupled mode with the *Pardiso* direct linear solver and *Jacobian* update on every iteration. Time stepping options depend on the solution scenario, but in most cases an initial step of 10 s and a maximum step of $5 \cdot 10^6$ s are appropriate values.

It should be noted, that in addition to these basic conservation equations a large overhead of specific equations is necessary for the definition of specific reservoir physics. These equations apply for the reservoir properties (porosity, two-phase permeability and capillary pressure), the physical property data of the components (gases, seawater, hydrates and sediment), mass and heat transfer data, thermodynamic equilibrium states (hydrate and gas/liquid thermodynamics) and kinetic expressions for hydrate decomposition and composition. These equations were clearly arranged in variable blocks and analytic functions, so the *COMSOL* model stays comprehensible and clearly documented for further work. In the scope presented here these important additional topics cannot be described in detail and are subject of further papers [6].

4. Simulation cases and results

The reference simulation case is the depressurization of a closed quadratic block with an edge length of 1000 m, a height of 20 m and a production well in the middle. Initial reservoir conditions are a pressure of 100 bar, a temperature of 10°C and a methane hydrate saturation of 40%. Well pressure is decreased to 30 bar and methane is produced over 15 years at constant pressure. For symmetry only 1/8 part of the whole system has to be calculated. Figs. 1a and 1b shows the temperature and hydrate distribution after 15 years of depressurization. Methane hydrate is fully decomposed near the well and to about 30% saturation far from the well. Gas saturation increases to about 25% in the upper part of the reservoir (not shown here).

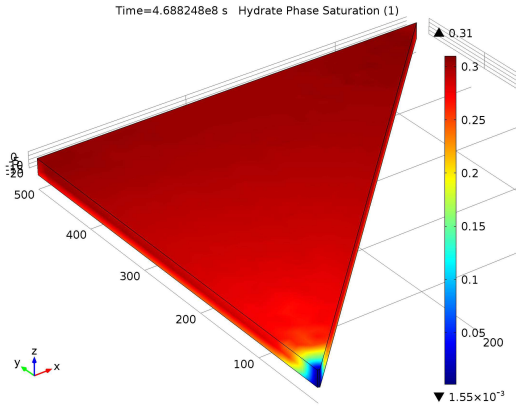

Figure 1a. Hydrate saturation distribution within a single layer hydrate system after 15 years of depressurization, 3d simulation, initial value 0.40

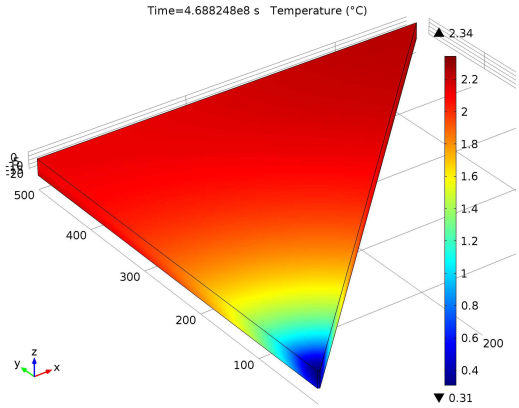

Figure 1b. Temperature distribution within a single layer hydrate system after 15 years of depressurization, 3d simulation, initial value 10°C

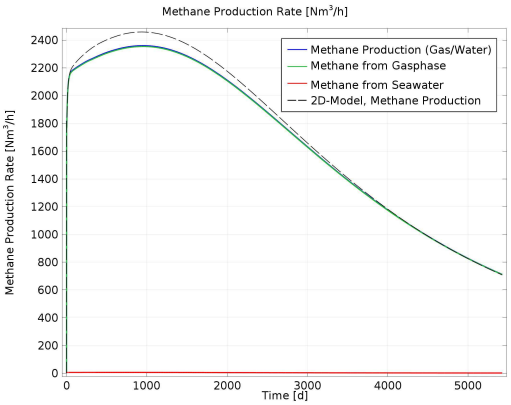

Figure 2. Methane production rate at the well vs. time for a period of 15 years

Due to hydrate decomposition heat the depressurization process approach to a nearly constant low reservoir temperature at about 1-2°C (this is the hydrate equilibrium temperature at 30 bar) and the decomposition ends here, because the reservoir is assumed to be thermally closed. Fig. 2 shows the methane production rate at the well vs. time for a production period of 15 years. For the assumed scenario a production over 2000 STD m^3/h can be realized for 7 years (depends on reservoir permeability assumptions). At later times the rate decreases as the system approach equilibrium.

A simulation case of more technical interest is the depressurization of a reservoir with an upper and lower burden and several hydrate layers embedded in sand/clay sections. Here, a reservoir with five methane hydrate layers (4 m in deep) interrupted by clay (8 m in deep) is simulated; the reservoir burden have a vertical size of 50 m. This very complex case is modelled in 2d axisymmetric. The distribution in methane hydrate saturation is shown in Fig. 3. Clearly the so-called *»fingering«* effect in hydrate saturation can be seen and the increased hydrate dissociation in the outer layers. Both are thermal effects due to heat conduction from the clay to the hydrate layers. The heat flux is maximal at the hydrate/clay interface, so the hydrate decomposition here is larger compared to inner regions.

An important feature of several small hydrate layers (so-called turbite layers) compared to one thick layer with same volume is the increase in methane production due to the thermal effects explained above. In Fig. 4, this effect is shown for simulations of 1, 2 and 5 hydrate layers.

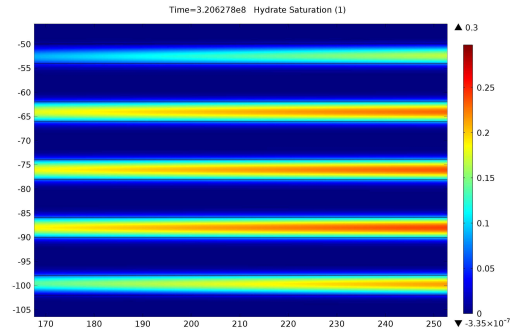

Figure 3. Hydrate saturation distribution within a 5-layer hydrate system after 10 years of depressurization, detail of a 2d axisymmetric model of a 1000 m in diameter reservoir

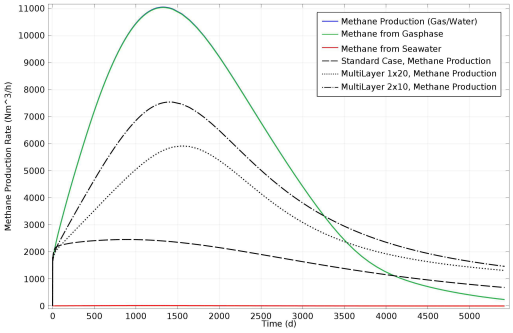

Figure 4. Methane production rate at the producer well, conditions as for Fig. 3, dotted/dashed curves for 1- and 2-layer systems and the reference single layer without any burden

The methane production rate increases with the number of layers and in the 5-layer system 11000 STD m^3/h are reached compared to 6000 STD m^3/h for a single layer system with burden and 2200 STD m^3/h for the reference system without any burden. It should be noted again, that the initial hydrate volume and the depressurization conditions are the same for all these cases.

One main goal of the *SUGAR* project is studying the methane production accompanied by a simultaneous CO_2 injection. The simulation case shown here is a 3-d model of a quadratic reservoir as given for Fig. 1, but with a production well and an injection well at opposite corners of the 1/8 geometric piece. This arrangement is symmetric too for alternating wells in horizontal alignment at a distance of 1000 m. Initial conditions are the same as in the reference case given before (single layer without any burden). The process starts with a pressure

decrease at the production well to 30 bar and a simultaneous injection of 2500 STD m^3/h CO_2 at the injection well.

The methane hydrate saturation after 15 years processing is given in Fig. 5a. Methane hydrate is decomposed in a large part of the volume around the injection well. This effect results from the embedded composing and decomposing kinetics of the CH_4/CO_2 system, which let methane hydrate decompose slowly at large CO_2 molar fractions in the gas phase.

In Fig. 5b the CO_2 hydrate saturation is shown for the same time stamp. CO_2 have formed hydrate in the area around the injection well which is free of methane hydrate now. It is noted here, that the amount of CH_4/CO_2 hydrate exchange strongly depends from kinetics and hydrate equilibrium parameters used in the reservoir model.

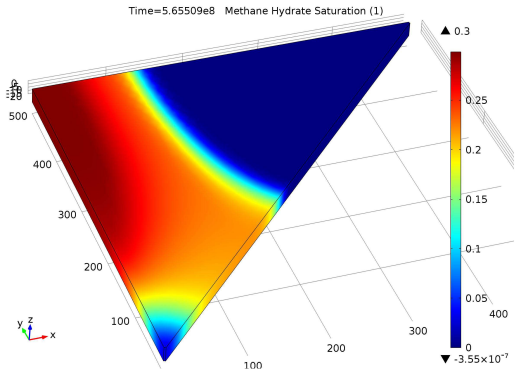

Figure 5a. Methane hydrate saturation after 15 years for a simultaneous 2-well production/injection study with injection of carbon dioxide, 3d model, depressurization and CH_4 production at lower left corner, CO_2 injection at upper right corner

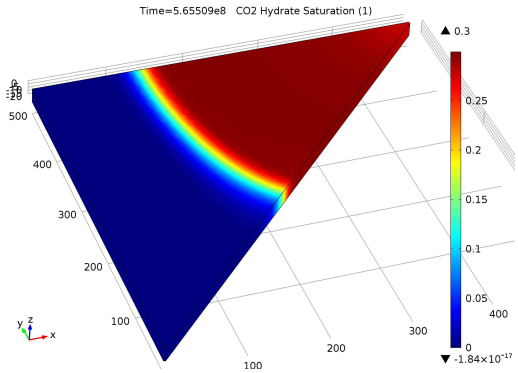

Figure 5b. CO_2 hydrate saturation after 15 years for a simultaneous 2-well production/injection study with injection of carbon dioxide (as for Fig. 5a)

The methane production rates of a depressurization process can be increased by a simultaneous CO_2 injection, as shown in Fig. 6. Here, the production rates at the producer well are given. Methane production (blue line) is increased after 2500 days (compare with Fig. 2) by the methane hydrate decomposition around the injection well. After 5000 days (13.5 years) first CO_2 is produced (green line), and at this point the production is to shut down if the emission of formerly injected CO_2 is unacceptable.

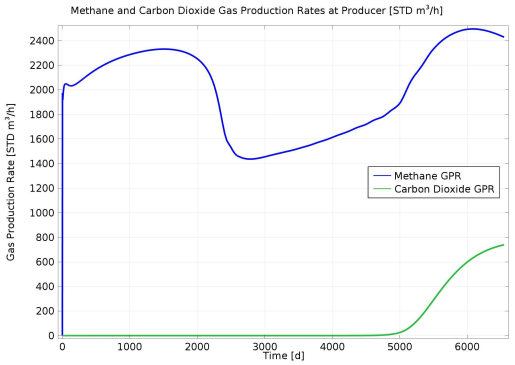

Figure 6. Methane and carbon dioxide production rates at the producer well, conditions as for Fig. 5, carbon dioxide break through after 5000 days

5. Conclusions

An immense amount of natural gas hydrates is presumed worldwide. The feasibility of methane recovery from hydrate deposits has already been proved in different numerical simulations and field tests. In addition, the feasibility of CO_2 sequestration by injecting it into hydrate reservoirs and building up CO_2 hydrate has been verified numerically and by means of laboratory tests so far. Within the scope of the German research project *SUGAR*, different technological approaches for the exploitation of natural gas hydrate deposits are evaluated and compared by means of dynamic system simulations and analysis.

The reservoir model developed with the help of *COMSOL Multiphysics* use a special total velocity approach to deal with a 2-phase Darcy flow in sediments partially filled with hydrates. The model simulate the time dependent evolution of pressure, temperature, gas, liquid and hydrate saturation, gas phase molar fractions and liquid phase concentrations. Important physical

effects like e.g. saturation dependent permeability, hydrate decomposition kinetics or solution of gases in seawater are taken into account. To cover a wide area of reservoir conditions and simulation cases, 3-d and 2-d axisymmetric model versions were developed and numerically parameterized in *COMSOL*.

The simulation cases shown here underline the big challenge and the scientific/technical chances of using reservoir models for such complex physical systems. Besides a reference case for studying basic properties of the system, more complex multi hydrate layer systems were simulated, and it can be shown that production rates can be enhanced significantly by reservoir immanent thermal effects. Methane production from hydrate can also be enhanced by the injection of carbon dioxide, and this is a promising result asking for more scientific efforts in future.

6. References

1. Sloan E.D.; Koh C.A.: Clathrate Hydrates of Natural Gases. Boca Raton, USA, CRC Press (2008)

2. Ota, M.; Abe, Y.; Watanabe, M.; Smith, R.L.; Inomata, H.: Methane Recovery from Methane Hydrate Using Pressurized CO2; Fluid Phase Equilibria 228-229 (2005)

3. Moridis, G.J.; Sloan, E.D.: Gas Production Potential of Disperse Low-Saturation Hydrate Accumulations in Oceanic Sediments, LBNL-5268, Lawrence Berkeley National Laboratory, Berkely, CA (2006)

4. Diaz-Viera, M.A.; Lopez-Falcon, D.A., Moctezuma-Bertier, A.; Ortiz-Tapia, A.: COMSOL Implementation of a Multiphase Fluid Flow Model in Porous Media, Proceedings of the COMSOL Conference 2008, Boston (2008)

5. Bundschuh, J.; Suarez-Arriaga, M; Samaniego, F.: Numerical Modeling of the Coupled Flow of Brine and Oil in Hydrocarbon Reservoirs; in: Numerical Modeling of Coupled Phenomena in Science and Engineering, CRC Press, London (2009)

6. Janicki, G.; Schlüter, S.; Hennig, T.; Deerberg, G.: Simulation of Methane Recovery from Gas Hydrates Combined with Storing Carbon Dioxide as Hydrates, Journal of Geological Research, doi:10.1155/2011/462156 (2011)

7. Acknowledgements

The support of our research activities by the German Federal Ministry of Economics and Technology (BMWi) and the German Federal Ministry of Education and Research (BMBF) is gratefully acknowledged.

8. Nomenclature

a	volumetric interface area, m^2/m^3
c	molar concentration, mol/m^3
c_p	specific heat capacity, J/(kg·K)
g	gravitational acceleration, m/s^2
Δh	latent heat, J/mol
k_{rel}	relative permeability, 1
K_f	intrinsic permeability, m^2
M	molar mass, kg/mol
P	pressure, Pa
q	heat source, W/m^3
R	composition rate, $mol/(m^3s)$
S	saturation, m^3/m^3
s	mass source, kg/m^3
$\tilde{s}$	molar source, mol/m^3
T	Temperature, K
u	Darcy velocity, m/s
y	molar fraction, mol/mol
β	volumetric expansivity, 1/K
χ	isothermal compressibility, 1/Pa
δ	diffusion coefficient, m^2/s
ε	artificial diffusion coefficient, m^2/s
ϕ	porosity, m^3/m^3
φ	composition derivation coefficient, 1
ψ	mass transfer coefficient, m/s
η	dynamic viscosity, Pa·s
Λ	hydraulic conductivity, 1/(Pa·s)
λ	heat conductivity, W/(m·K)
ν	hydrate number
ρ	specific density, kg/m^3
$\tilde{\rho}$	molar density, mol/m^3

Indices

*	in phase equilibrium
abs	absorption
C	CO_2 / capillary pressure
CH	CO_2 hydrate
G	gas phase
H	hydrate phase
i	component i
j	phase j
L	liquid phase
M	methane
MH	methane hydrate
n	inert gas component n
rel	relative
S	sediment phase